Probing of the pseudogap via thermoelectric properties in the Au-Al-Gd quasicrystal approximant

Asuka Ishikawa,[1] Yoshiki Takagiwa,[2] Kaoru Kimura,[3] and Ryuji Tamura[1]
[1]*Department of Materials Science and Technology, Tokyo University of Science, Katsushika, Tokyo 125–8585, Japan*
[2]*National Institute of Materials Science, Tsukuba, Ibaraki 305-0047, Japan*
[3]*Department of Advanced Materials Science, the University of Tokyo, Kashiwa, Chiba 277–8561, Japan*
(Received 11 July 2016; revised manuscript received 25 January 2017; published 6 March 2017)

The pseudogap of the recently discovered Au-Al-Gd quasicrystal approximant crystal (AC) is investigated over a wide electron-per-atom (e/a) ratio of ∼0.5 using thermoelectric properties as an experimental probe. This Au-Al-Gd AC provides an ideal platform for fine probing of the pseudogap among a number of known ACs because the Au-Al-Gd AC possesses an *extraordinarily* wide single-phase region with respect to the variation in the electron concentration [A. Ishikawa, T. Hiroto, K. Tokiwa, T. Fujii, and R. Tamura, Phys. Rev. B **93**, 024416 (2016)], in striking contrast to, for instance, binary stoichiometric Cd_6R ACs. As a result, a salient peak structure is observed in the Seebeck coefficient, S, with the composition as well as that of the power factor $S^2\sigma$, in addition to a gradual variation in the conductivity, σ, and S. These two features are directly associated with rapid and slow variations, respectively, of spectral conductivity $\sigma(E)$, and hence the fine structure inside the pseudogap, in the vicinity of the Fermi level E_F. Based on the observed continuous variation of the Fermi wave vector reported in the previous experimental work, fine tuning of E_F toward an optimal position was attempted, which led to the successful observation of a sharp peak in $S^2\sigma$ with a value of $\sim 270\,\mu W/m \cdot K^2$ at 873 K. This is the highest value ever reported among both Tsai-type and Bergman-type compounds. The dimensionless figure of merit was determined as 0.026 at 873 K, which is also the highest reported among both Tsai-type and Bergman-type compounds.

DOI: 10.1103/PhysRevB.95.104201

I. INTRODUCTION

The existence of a pseudogap in the vicinity of the Fermi level E_F is one of the characteristic features of quasicrystals (QCs) [1,2] and related approximant crystals (ACs) [3]. The first-principles band structure calculation on the Al-Mn-Si AC by Fujiwara [4] and Fujiwara and Yokokawa [5] provided the first theoretical evidence of the pseudogap formation in QCs. The existence of a pseudogap was immediately supported by the observations of small electronic specific heat coefficients, much smaller than the free electron value [6,7]. Subsequent photoelectron spectroscopy studies then provided direct experimental evidence for the pseudogap formation near E_F for the Al-Cu-Fe and Al-Pd-Mn QCs [8] and the Cd-Ca QC and AC [9]. Optical conductivity [10] and time-resolved photo-induced optical reflectivity [11] measurements and scanning tunneling spectroscopy [12] have also been employed to probe the pseudogap in the density of states (DOS) near E_F. Such pseudogap formation near E_F in QCs and ACs has caught particular interest in view of thermoelectric materials, and relatively high power factors reflecting the pseudogap have been reported in the literature [13–23].

Ishikawa *et al.* [24] recently discovered the first composition-driven spin glass to ferromagnetic transition in a Tsai-type AC, i.e., Au-Al-Gd AC, the cluster structure of which is schematically depicted in Fig. 1. A striking feature of the Au-Al-Gd AC is that it has an *extraordinarily* wide single-phase region with $x = 14-37$ in $Au_{86-x}Al_xGd_{14}$ [24], which is in a sharp contrast with, for instance, the binary stoichiometric Cd_6R ACs. The composition-driven magnetic transition was attributed to the oscillating Ruderman-Kittel-Kasuya-Yosida (RKKY) interaction. Figure 2 shows the composition dependence of the lattice parameter and the paramagnetic Curie temperature of $Au_{86-x}Al_xGd_{14}$, with $x = 14-37$ as a function of the Al concentration, x. The systematic change in the lattice parameter clearly shows the existence of a wide single-phase region with the huge variation of x over 23 at. %. The observed oscillation of the paramagnetic Curie temperature indicates a continuous variation in the Fermi wave vector, k_F, over the widely elongated single-phase region, which is brought about by the change in the Au/Al composition. Thus, the Au-Al-Gd AC provides an ideal platform for probing of the pseudogap structure via the continuous variation of E_F. We present herein a thorough investigation on the pseudogap via the electron concentration dependence of the thermoelectric properties of the Au-Al-Gd AC. We also show the occurrence of a distinct anomaly in both the Seebeck coefficient and the power factor, the origin of which will be discussed in terms of the energy dependence of the spectral conductivity $\sigma(E)$ based on a phenomenological argument.

II. EXPERIMENTAL

Samples with nominal compositions of $Au_{86-x}Al_xGd_{14}$ ($x = 14-37$) were prepared by arc melting followed by remelting in an induction furnace, both under an argon atmosphere. Details of the sample preparation and phase characterization are described elsewhere [24]. For $Au_{52}Al_{34}Gd_{14}$, a powder sample was sintered using a spark plasma sintering instrument (SPS-515S; Fuji Electronic Industrial Co., Kanagawa, Japan) to prepare a sample suitable for thermal conductivity measurements. The sintering temperature was 1140 K, and the sample was held for 20 minutes under a uniaxial pressure of 57 MPa in an argon atmosphere. The obtained bulk sample was confirmed to be single phase (Fig. 3) and had a relative density of 85%, which is suitable for thermal conductivity measurements.

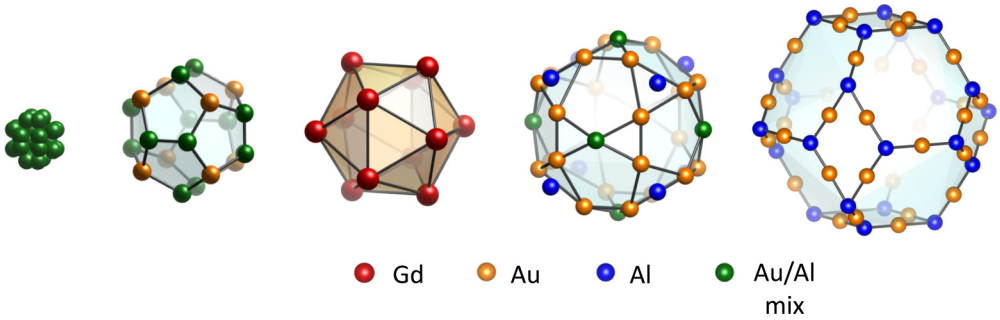

FIG. 1. The Tsai-type icosahedral cluster in the Au-Al-Gd 1/1 AC drawn schematically by assuming the structural model of the Au-Al-Yb 1/1 AC [25]. The clusters form a bcc lattice in the AC.

Electrical conductivity and Seebeck coefficient measurements were conducted using the four-probe method and the steady-state temperature gradient method, respectively, with a Seebeck coefficient/electric resistance measurement system (ZEM–1, Advance-Riko, Inc., Kanagawa, Japan). The thermal conductivity was determined using the equation $\kappa_{\text{total}} = d \cdot C_p \cdot \lambda$, where d, C_p, and λ are the density, specific heat, and thermal diffusivity, respectively. Both C_p and λ were measured with the laser flash method (TC–7000; Advance-Riko, Inc.). All measurements were performed at temperatures between 373 and 873 K.

III. RESULTS AND DISCUSSION

A. Electrical conductivity and Seebeck coefficient of the Au-Al-Gd AC

Figures 4(a) and 4(b) show the temperature dependence of σ and S for a series of $Au_{86-x}Al_xGd_{14}$ ($x = 14-37$) ACs, respectively. Both σ and S increase with the temperature above 373 K over the entire single-phase region. The positive temperature coefficients of σ, which is opposite to that for typical crystalline metals, are one of the characteristic features of QCs and ACs. Here, we note that for a crystalline material, such increases in σ with temperature cannot be accounted for by the scattering of conduction electrons, which would otherwise decrease σ with temperature. On the other hand, the sign of S remains positive over the entire single-phase region, which means that in the Au-Al-Gd AC, E_F is always located in an energy region in which the density of states or the spectral conductivity has a negative slope. Similar behavior has also been observed in Au-Al-RE(RE = Yb,Tb,Gd) QCs and ACs [26]. The values of σ and S in Figs. 4(a) and 4(b) are strongly dependent on the composition; σ varies over one order of magnitude from 600 $(\Omega\,\text{cm})^{-1}$ to 7000 $(\Omega\,\text{cm})^{-1}$ at 373 K as x changes, while S varies between 0 and 18 μV/K at 373 K. Such a salient composition dependence is reminiscent of the behaviors observed in some Al-based icosahedral QCs, such as Al-Pd-Re [16], Al-Ga-Pd-Re [23], and in the Tsai-type Au-Al-Yb AC [26], which is attributed to the formation of a (deep) pseudogap in the vicinity of E_F.

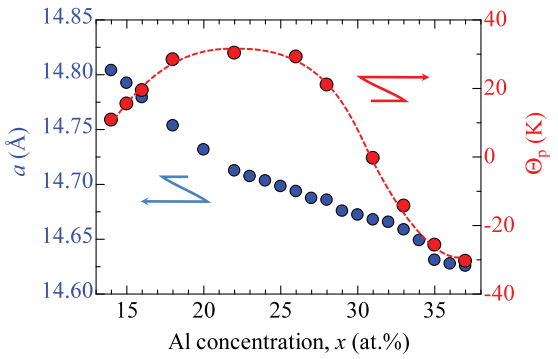

FIG. 2. Lattice parameter, a, and paramagnetic Curie temperature, Θ_p, as a function of the Al concentration, x, for $Au_{86-x}Al_xGd_{14}$ ($x = 14-37$).

B. Phenomenological argument of the electrical conductivity and Seebeck coefficient of the Au-Al-Gd AC

Figure 5(a) shows σ and S at 373 K as a function of the Al concentration x, for $Au_{86-x}Al_xGd_{14}$ with $x = 14-37$. The $\sigma_{373\,K}$ exhibits a general trend to decrease with increasing x, while $S_{373\,K}$ increases slowly first and then rapidly at higher Al concentrations to exhibit a peak at ~35 at. %. According to the Mott formula, the electrical conductivity and Seebeck

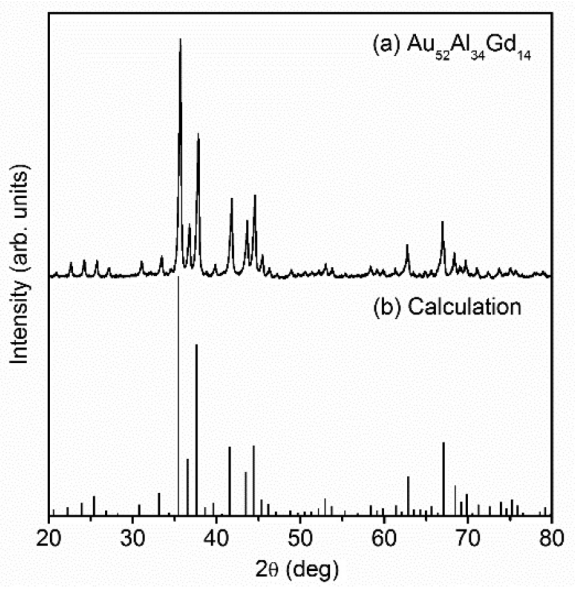

FIG. 3. (a) Cu $K\alpha$ powder x-ray diffraction pattern of the sintered $Au_{52}Al_{34}Gd_{14}$ AC and (b) simulated diffraction pattern using the structural model of Au-Al-Yb AC [25].

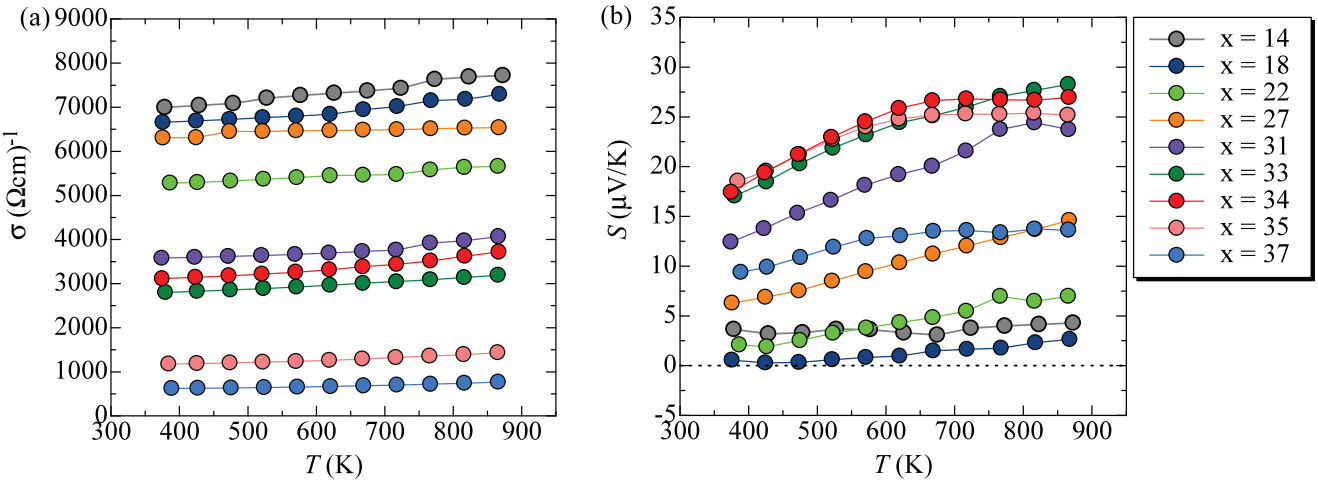

FIG. 4. (a) Electrical conductivity, σ, and (b) Seebeck coefficient, S, as a function of temperature for $Au_{86-x}Al_xGd_{14}$ ($x = 14$–37).

coefficient are expressed by the following formulae:

$$\sigma = \int \sigma(E)(-\partial f/\partial E)dE, \quad (1)$$

$$S = -\frac{1}{\sigma eT}\int \sigma(E)(E-\mu)(-\partial f/\partial E)dE, \quad (2)$$

where $\sigma(E)$ is the spectral conductivity, f is the Fermi-Dirac distribution function, and μ is the chemical potential. Here we note that Pierce *et al.* used the same formula in interpreting the thermoelectric properties of Al-based QCs [27]. In contrast to the previous analyses, we have not made any assumptions to elucidate $\sigma(E)$, such as (1) a temperature-independent E_F or (2) a symmetrical form of the DOS around E_F. According to Eq. (2), the composition dependence of S can be attributed to either or both of the two factors: σ in the denominator and the integral in the numerator. The latter can also be expressed as σS. To determine which factor is responsible for the observed feature in S, both σ and σS are plotted as a function of the Al concentration in Fig. 5(b). The observed maximum of S around 35 at. % is considered to be a consequence of the maximum in σS around 34 at. %, which indicates that *the anomaly in S is due to strong asymmetry of the spectral conductivity* $\sigma(E)$ *at* $E = \mu(373\,\mathrm{K})$.

To obtain insight into the energy dependence of $\sigma(E)$ near the anomaly, we neglect the temperature dependence of $\sigma(E)$ and assume that the functional of $\sigma(E)$ can be expanded in a power series of E around $E = \mu(T) \equiv \mu$, as

$$\sigma(E) = \alpha(T) + \beta(T)(E-\mu) + \gamma(T)(E-\mu)^2 + \delta(T)(E-\mu)^3 + \ldots \quad (3)$$

Under these assumptions, σS can be evaluated as

$$\sigma S = -\frac{\pi^2}{3e}k_B^2\beta(T)T - \frac{7\pi^4}{15e}k_B^4\delta(T)T^3 + O(T^5). \quad (4)$$

We note that T-linear dependence is observed when the higher order terms in Eq. (4), i.e., $O(T^3)$, is negligible, and in this case σS simply takes the form of $\sigma S = -\frac{\pi^2}{3e}k_B^2\beta(T)T$. Figure 6 shows σS as a function of T for compositions in the vicinity of 35 at. % Au. All the data are fairly well aligned on straight lines drawn from the origin below ~600 K. Such behavior can be explained by the first term in Eq. (4), when the temperature dependence of $\beta(T)$ is negligible. Thus, the

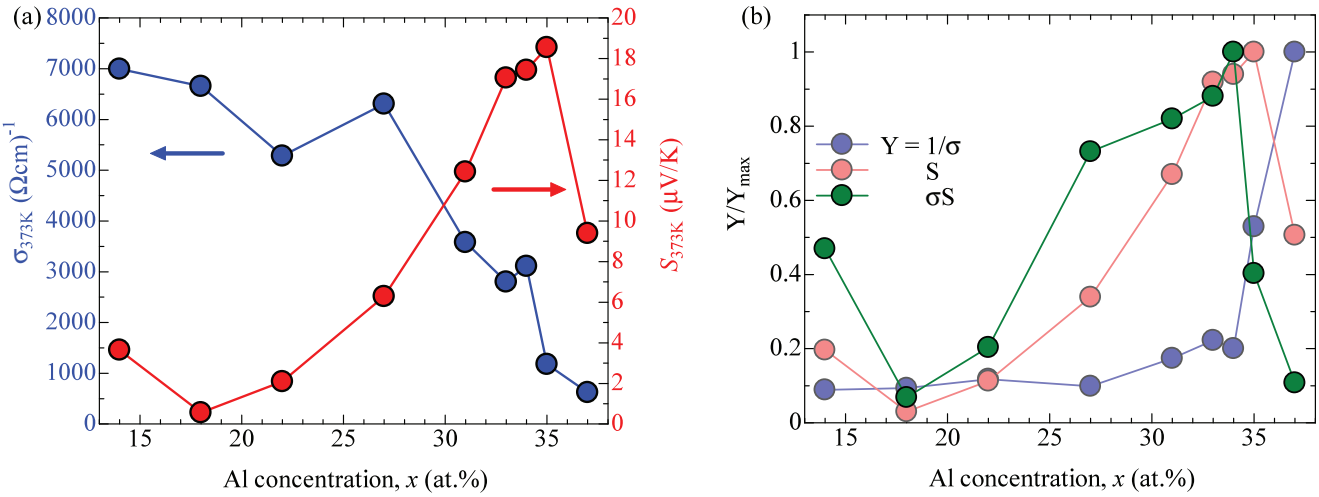

FIG. 5. (a) Electrical conductivity, σ, Seebeck coefficient, S, and (b) Y/Y_{max} ($Y = 1/\sigma$, S, σS) at 373 K as a function of the Al concentration, x, for $Au_{86-x}Al_xGd_{14}$ ($x = 14$–37).

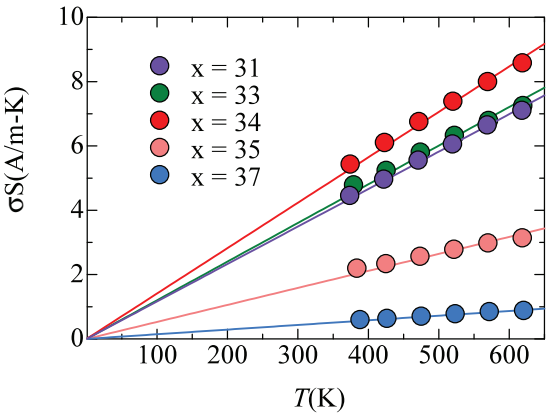

FIG. 6. The σS as a function of temperature, T, for the compositions in the vicinity of 35 at. % Au in $Au_{86-x}Al_xGd_{14}$.

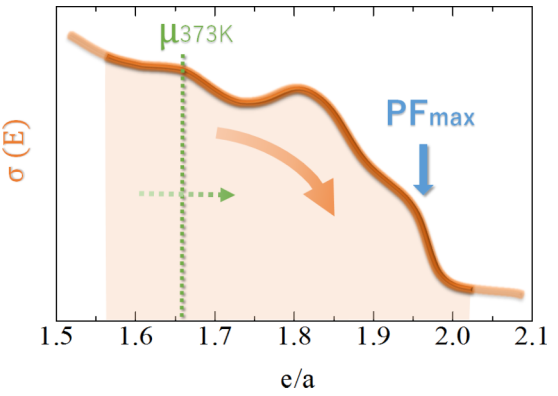

FIG. 7. The pseudogap profile in terms of the spectral conductivity $\sigma(E)$ inferred from obtained $\sigma_{373\,K}$ and $S_{373\,K}$, as a function of the electron-per-atom (e/a) ratio for the Au-Al-Gd AC. μ_{373K} denotes the chemical potential at 373 K.

composition dependence of σS is attributed to the variation in the slope of $\sigma(E)$ at $E = \mu$, i.e., $d\sigma(E)/dE|_{E=\mu}$, and the observed peak in S is understood as a consequence of the maximum in $d\sigma(E)/dE|_{E=\mu}$ with the variation of x in $Au_{86-x}Al_xGd_{14}$. Here, an increase in x causes an increase in k_F, i.e., a shift of E_F toward higher energies, as recently verified experimentally [24]. We note that such a rapid variation in $\sigma(E)$ at ∼34 at.% Au is also consistent with the rapid decrease in $\sigma_{373\,K}$ observed at ∼34 at.% Au, which implies the existence of a fine structure inside the pseudogap. Figure 7 schematically depicts the pseudogap profile in terms of $\sigma(E)$, which is inferred from the obtained $\sigma_{373\,K}$ and $S_{373\,K}$ values, as a function of the electron-per-atom (e/a) ratio for the Au-Al-Gd AC, where the number of the valence electrons are assumed to be +1 and +3 for Au and Al, respectively. We note that measurement of the specific heat is necessary in order to obtain direct information on the DOS [17,28,29].

Figure 8 shows the temperature dependence of the power factor, $S^2\sigma$, for a series of Au-Al-Gd ACs. The $S^2\sigma$ increases monotonically with increasing temperature for all of the compositions, which is in sharp contrast with the Mackay icosahedron (MI)-type QCs and ACs. The Seebeck coefficient can be approximated as $S \cong -\frac{\pi^2}{3e\sigma}k_B^2\beta T$ below ∼600 K from the above argument; therefore, the power factor is given by $S^2\sigma \cong \frac{\pi^4}{9e^2\sigma(T)}k_B^4\beta^2T^2$. The increasing trend of $S^2\sigma$ above 373 K in the Tsai-type AC is thus understood to be partly due to the small temperature increases of $\sigma(T)$. Figure 8(b) shows that optimization of the magnitude of k_F via the Au/Al compositions leads to a significant enhancement as well as a salient maximum in the power factor. The maximum power factor is obtained as $\sim 270\,\mu W/m \cdot K^2$ at 873 K for $x = 34$, which is the highest known value among both the Tsai-type and Bergman-type compounds [26]. Moreover, it even exceeds that of the Al-Ga-Pd-Mn QC [30] above ∼850 K, which has the highest zT among all QCs and ACs.

Figure 9 shows the temperature dependence of κ_{total} and κ_{phonon} for a sintered sample at the optimized composition of $x = 34$. Here, κ_{phonon} is estimated by assuming the Wiedemann–Franz law, i.e., $\kappa_{phonon} = \kappa_{total} - \kappa_{electron} = \kappa_{total} - L\sigma T$, where L is the Lorenz number (degenerate limit: $2.44 \times 10^{-8}\,W\,\Omega/K^2$). The monotonic increase of κ_{total} for the Au-Al-Gd AC is attributed to an increase of $\kappa_{electron}$. On the other hand, κ_{phonon} is extremely low and shows a glasslike value of $\sim 1\,W/m \cdot K$. We note that the value of κ_{phonon} is distinctly lower than those of other Tsai-type and

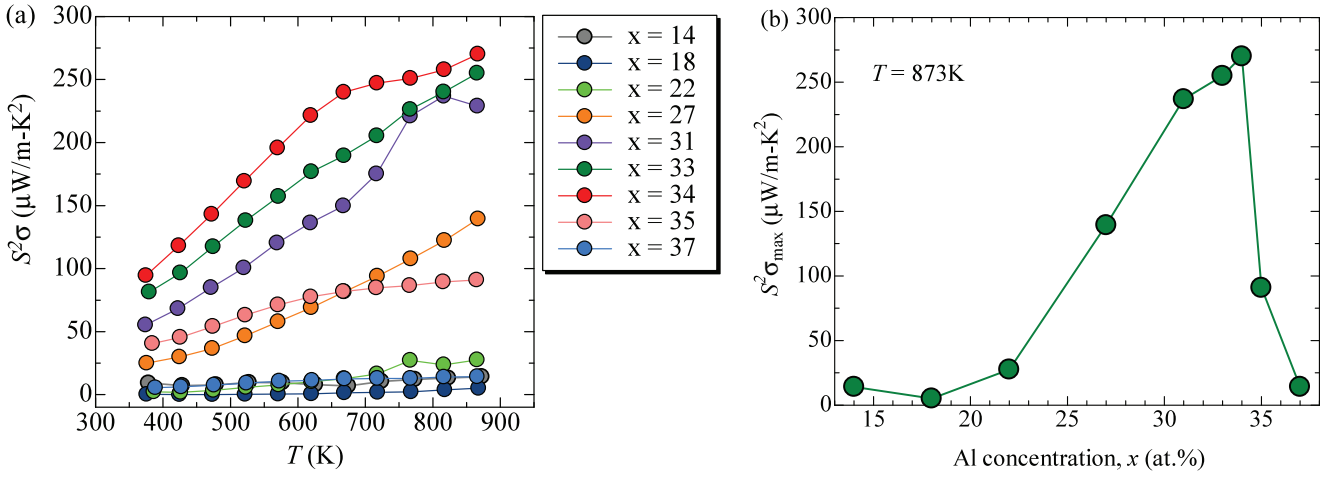

FIG. 8. Power factor, $S^2\sigma$, as a function of (a) temperature and (b) the Al concentration, x, for $Au_{86-x}Al_xGd_{14}$ ($x = 14-37$).

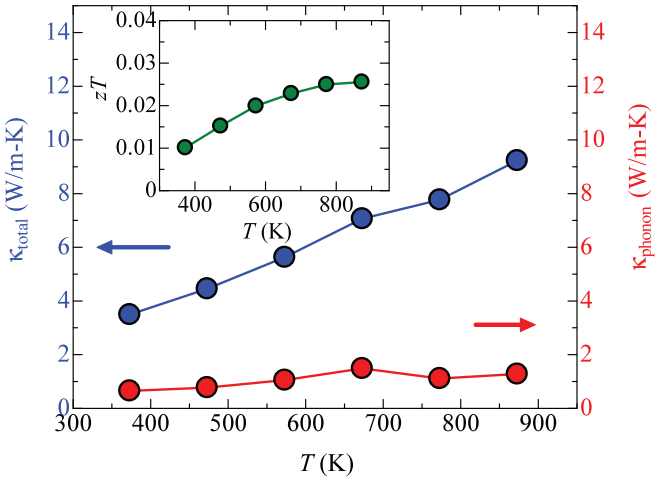

FIG. 9. Total thermal conductivity, κ_{total}, and phonon thermal conductivity, κ_{phonon}, for $Au_{52}Al_{34}Gd_{14}$, which has the largest power factor. The inset shows the dimensionless figure of merit, ZT, as a function of temperature for $Au_{52}Al_{34}Gd_{14}$.

Bergman-type compounds, which indicates that the heavy masses of Au and Gd also contribute to the very low κ_{phonon}, in addition to the existence of mixed and partially occupied atomic sites. The inset of Fig. 9 shows zT as a function of temperature for $x = 34$. The maximum zT value reaches 0.026 at 873 K, which is significantly higher than the highest value reported for Tsai-type compounds to date, i.e., Au-Al-Yb [26].

IV. CONCLUSIONS

The pseudogap profile of the Au-Al-Gd AC was closely investigated by the electrical conductivity, σ, and the Seebeck coefficient, S, over an *extraordinarily* wide composition range of 23 at. % at temperatures in the range of 373–873 K. Both systematic and anomalous changes in σ and S were observed with variation of x in $Au_{86-x}Al_xGd_{14}$ ($x = 14-37$), both of which are attributed to slow and rapid variation of the spectral conductivity as a function of energy, respectively. Fine tuning of σ and S by shifting E_F to an optimal energy position was attempted, which led to the observation of a salient maximum in the power factor with a value of $\sim 270\,\mu W/m \cdot K^2$ at 873 K for the $Au_{52}Al_{34}Gd_{14}$ AC. The dimensionless figure of merit zT reached 0.026 at 873 K for the optimized composition, which, to the best of our knowledge, is the highest recorded value among both Tsai-type and Bergman-type compounds.

ACKNOWLEDGMENTS

This work was supported by the Japan Society for the Promotion of Science (JSPS) through KAKENHI Grants No. JP26709051 and No. JP16H04018.

A.I. and Y.T. contributed equally to the paper.

[1] D. Shechtman, I. Blech, D. Gratias, and J. W. Cahn, Phys. Rev. Lett. **53**, 1951 (1984).
[2] D. Levine and P. J. Steinhardt, Phys. Rev. Lett. **53**, 2477 (1984).
[3] V. Elser and C. L. Henley, Phys. Rev. Lett. **55**, 2883 (1985).
[4] T. Fujiwara, Phys. Rev. B **40**, 942 (1989).
[5] T. Fujiwara and T. Yokokawa, Phys. Rev. Lett. **66**, 333 (1991).
[6] K. Kimura, H. Iwahashi, T. Hashimoto, S. Takeuchi, U. Mizutani, S. Ohashi, and G. Itoh, J. Phys. Soc. Jpn. **58**, 2472 (1989).
[7] U. Mizutani, Y. Sakabe, T. Shibuya, K. Kishi, K. Kimura, and S. Takeuchi, J. Phys.: Condens. Matter **2**, 6169 (1990).
[8] Z. M. Stadnik, D. Purdie, M. Garnier, Y. Baer, A. P. Tsai, A. Inoue, K. Edagawa, S. Takeuchi, and K. H. J. Buschow, Phys. Rev. B **55**, 10938 (1997).
[9] R. Tamura, T. Takeuchi, C. Aoki, S. Takeuchi, T. Kiss, T. Yokoya, and S. Shin, Phys. Rev. Lett. **92**, 146402 (2004).
[10] C. C. Homes, T. Timusk, X. Wu, Z. Altounian, A. Sahnoune, and J. O. Ström-Olsen, Phys. Rev. Lett. **67**, 2694 (1991).
[11] T. Mertelj, A. Ošlak, J. Dolinšek, I. R. Fisher, V. V. Kabanov, and D. Mihailovic, Phys. Rev. Lett. **102**, 086405 (2009).
[12] R. Widmer, P. Gröning, M. Feuerbacher, and O. Gröning, Phys. Rev. B **79**, 104202 (2009).
[13] A. L. Pope, T. M. Tritt, M. A. Chernikov, and M. Feuerbacher, Appl. Phys. Lett. **75**, 1854 (1999).
[14] E. Maciá, Appl. Phys. Lett. **77**, 3045 (2000).
[15] E. Maciá, Phys. Rev. B **64**, 094206 (2001).
[16] K. Kirihara and K. Kimura, J. Appl. Phys. **92**, 979 (2002).
[17] T. Takeuchi, T. Otagiri, H. Sakagami, T. Kondo, U. Mizutani, and H. Sato, Phys. Rev. B **70**, 144202 (2004).
[18] Y. K. Kuo, K. M. Sivakumar, H. H. Lai, C. N. Ku, S. T. Lin, and A. B. Kaiser, Phys. Rev. B **72**, 054202 (2005).
[19] E. Maciá, Phys. Rev. B **80**, 205103 (2009).
[20] M. Bobnar, S. Vrtnik, Z. Jagličić, M. Wencka, C. Cui, A. P. Tsai, and J. Dolinšek, Phys. Rev. B **84**, 134205 (2011).
[21] E. Maciá, Crit. Rev. Solid State Mater. Sci. **37**, 215 (2012).
[22] Y. Takagiwa and K. Kimura, Sci. Technol. Adv. Mater. **15**, 044802 (2014).
[23] Y. Takagiwa, T. Kamimura, J. T. Okada, and K. Kimura, Mater. Trans. **55**, 1226 (2014).
[24] A. Ishikawa, T. Hiroto, K. Tokiwa, T. Fujii, and R. Tamura, Phys. Rev. B **93**, 024416 (2016).
[25] T. Ishimasa, Y. Tanaka, and S. Kashimoto, Philo. Mag. **91**, 4218 (2011).
[26] Y. Takagiwa, K. Kimura, K. Sawama, T. Hiroto, K. Nishio, and R. Tamura, J. Alloys Compds. **652**, 139 (2015).
[27] F. S. Pierce, S. J. Poon, and B. D. Biggs, Phys. Rev. Lett. **70**, 3919 (1993).
[28] T. Takeuchi, T. Onogi, S. Otagiri, U. Mizutani, H. Sato, K. Kato, and T. Kamiyama, Phys. Rev. B **68**, 184203 (2003).
[29] E. Macia, T. Takeuchi, and T. Otagiri, Phys. Rev. B **72**, 174208 (2005).
[30] Y. Takagiwa, T. Kamimura, S. Hosoi, J. T. Okada, and K. Kimura, J. Appl. Phys. **104**, 073721 (2008).